A Molecular Dynamics Study of the Decane/Water Interface

Aldert R. van Buuren, Siewert-Jan Marrink, and Herman J. C. Berendsen*

BIOSON Research Institute and Laboratory of Biophysical Chemistry, University of Groningen, Nijenborgh 4, 9747 AG Groningen, The Netherlands

Received: April 6, 1993; In Final Form: June 13, 1993

Several molecular dynamics simulations on the interface between liquid decane and liquid water have been performed with the purpose to study the sensitivity of surface properties to the van der Waals parameters. The models used consisted of 50 decane molecules and 389 water molecules in a two-phase system. By changing the van der Waals parameters, i.e., varying the Lennard-Jones parameters ϵ and σ between the united CH_2 and CH_3 atoms of the decane molecules and the O atom of the water molecules, sharper interfaces were obtained. The excess free energy of water in decane and the surface tension between water and decane are presented for the van der Waals parameters used. From comparison to experimental values for the solubility of water in decane and the surface tension, the best parameters within the tested sets are when using the SPC/E water model: ϵ_{O-CH_3} = 0.849 kJ/mol, ϵ_{O-CH_2} = 0.706 kJ/mol, and σ_{O-C} = 0.344 nm. When using the SPC water model, the best parameters are ϵ_{O-CH_3} = 0.637 kJ/mol, ϵ_{O-CH_2} = 0.529 kJ/mol, and σ_{O-C} = 0.344 nm. We also evaluated differences between the interfacial and bulk liquids. At the interface, water showed an orientational preference, whereas the decane molecules were more laterally oriented with respect to the interface.

Introduction

In this report we present the results of molecular dynamics calculations on an oil/water interface. It is important from both a technical and a theoretical point of view to gain detailed insight into the properties of liquid/liquid interfaces; they play an important role in surface science and surfactant behavior. Numerous computer simulations on the liquid/vapor interfaces have been reported,[1-8] but until recently only a few theoretical studies of liquid/liquid interfaces have appeared in the literature.[9-14] Carpenter and Hehre reported a MD study of the hexane/water interface.[12] The interface was found to be 1.0 nm wide and not to be molecularly sharp. They also observed a small number of hexane molecules completely surrounded by water, which is not consistent with the known solubility of hexane in water, and believed it to be an artifact of the intermolecular potentials used. (They used standard SPC[15] and OPLS[16] parameters.) Meyer et al.[13] used two identical Lennard-Jones liquids to investigate two immiscible liquids. They calculated the interactions between two atom types L1 and L2 by using modified Lennard-Jones potential functions so they could vary the miscibility of the liquids. Their main conclusion was that reducing the attractive part of the potential leads to a reduced miscibility.

In previous simulations involving alkane chains[33-35] we have used Rykaert–Bellemans potentials[20] for dihedral angles and methylene Lennard-Jones interactions, with adjusted values[33] for the methyl parameters. These Lennard-Jones parameters were combined with the "hydrophobic values" of the water oxygen, as used in GROMOS.[17] The present investigation was prompted by the observation that this force field did not yield correct interface behavior. In the simulations of surfactant/oil/water systems, it appeared that the solubility of decane in water was far too high. We decided to perform a set of simulations to optimize the intermolecular potential parameters. To investigate the detailed structure of the decane/water interface, we have selected a number of properties which are characteristic for the interactions between the liquids: density and pressure profiles, surface tension, ordering of the molecules near the interface,[10,12,14,18] and free energy of solvation. These characteristics are analyzed for a number of different force field parameters. When the van der Waals parameters between molecules of two immiscible liquids are changed, not only the interaction energy between the two liquids but also the density and pressure profiles at the interface will change. By calculating the free energy of water in the bulk oil phase, one can compute the solubility of water in decane. Higher repulsion between the C atoms of decane and the O atoms of water will give a lower solubility for water in decane and result in a sharper interface. It will also have an effect on the ordering of the water and oil molecules near the interface. When the interface becomes sharper, the water molecules near the interface will form ordered layers and the decane molecules will become more laterally oriented with respect to the interface. All these characteristics will give information about the relation between the van der Waals parameters and the macroscopic properties of the interface. We expect that the described properties are most sensitive to the parameter $\epsilon_{(C-O)}$.

Methods

A series of molecular dynamics simulations was performed on the decane/water interface using a (periodic) box that contained 50 molecules of *n*-decane and 389 molecules of SPC/E water.[19]

Force Field. The configurational energies and forces were computed with the GROMOS87[17] package. The energy of a molecular system is described by simple potential energy functions comprising stretch, bend, torsional, Lennard-Jones, and electrostatic interactions. For the dihedrals $CH_2CH_2CH_2CH_2$ and $CH_2CH_2CH_2CH_3$ the Ryckaert–Bellemans potential[20] was used (which gives better statistics on trans/gauche behavior)

$$V(\psi) = \sum_{i=0}^{5} C_i(\cos \psi)^i \qquad (1)$$

with C_i (i = 0, ..., 5) = 9.28, 12.16, −13.12, −3.06, 26.24, and −31.5 kJ/mol. The use of this potential implies exclusions of Lennard-Jones interactions between the first and last atom of the dihedral, and ψ is defined according to the polymer convention ($\psi_{trans} = 0$). The methylene and methyl Lennard-Jones parameters were taken from ref 33.

The molecular model that is used treats all atoms explicitly, except for the hydrogen atoms that are bound to carbon atoms. The CH_n atoms (n = 1, 2, or 3) are treated as united atoms, and no special hydrogen-bond potential has been included. For the nonbonded interactions between sites i and j, the simple functional

0022-3654/93/2097-9206$04.00/0

TABLE I: Molecular Geometries,[a] Partial Charges,[b] and Lennard-Jones Parameters[c]

molecule		value	molecule		value
decane	r(C–C)	0.153	water	r(O–H)	0.100
	∠(C–C–C)	111.0		∠(H–O–H)	109.5
	q(CH_3)	0.0		q(O)	–0.8476
	q(CH_2)	0.0		q(H)	+0.4238
	ϵ(CH_3)	0.6243		ϵ(O)[d]	2.31
	ϵ(CH_2)	0.4301		σ(O)[d]	0.256
	σ(CH_3)	0.374		ϵ(O)[e]	0.650
	σ(CH_2)	0.374		σ(O)[e]	0.317

[a] Bond lengths in nanometers; bond angles in degrees. [b] q in electrons. [c] ϵ in kJ/mol and σ in nm. [d] Hydrophobic Lennard-Jones parameters as used in the GROMOS force field for O_{water}–C interactions. [e] Values for SPC(/E) water, also referred to as hydrophilic parameters in GROMOS.

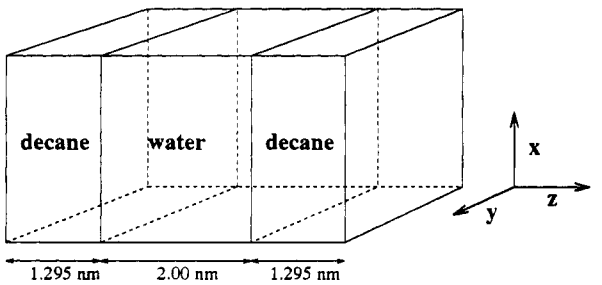

Figure 1. Initial configuration. Water is in the middle, and decane is on both the left and right side of the box. The z axis is chosen to be perpendicular to the interface.

form is used

$$V_{ij} = \frac{q_i q_j}{4\pi\epsilon_0 r_{ij}} + \frac{A_{ij}}{r_{ij}^{12}} - \frac{C_{ij}}{r_{ij}^{6}} \qquad (2)$$

q_i is the charge on site i, r_{ij} is the distance between the sites, and A and C are the van der Waals parameters ($A_{ii} = 4\epsilon_i\sigma_i^{12}$ and $C_{ii} = 4\epsilon_i\sigma_i^{6}$). The van der Waals parameters between different sites are given by the combination rules[16] $A_{ij} = (A_{ii}A_{jj})^{1/2}$ and $C_{ij} = (C_{ii}C_{jj})^{1/2}$. The GROMOS force field uses a different A_{OO} for the O_{water}–C and O_{water}–O_{water} interaction, indicated in Table I as hydrophobic and hydrophilic value, respectively.

The Model. The initial configuration of 50 decane molecules and 389 water molecules was constructed by building two opposite monolayers of decane with a distance of 2.0 nm in between (Figure 1). Each monolayer contained 25 decane molecules, initially in the all-trans configuration and randomly rotated around their head-to-tail axis. The distance between the layers was filled with SPC/E[16] water, using a cubic box containing 216 equilibrated SPC/E water molecules as a building block. The water molecules were able to penetrate the layers by 0.1 nm while keeping a minimum distance of 0.23 nm from the atoms of the decane molecules. The dimensions of the box were 2.50 nm × 2.50 nm × 4.589 nm, leading to a total density of 1.0 g/cm³ for the water phase and 0.73 g/cm³ for the oil phase. Periodic boundary conditions were applied in all three spatial dimensions. The model

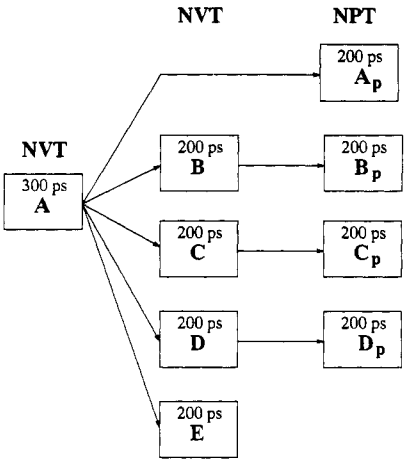

Figure 2. Schematic representation of the MD simulations performed.

geometries, partial charges, and Lennard-Jones parameters, as used in all simulations, are given in Table I.

To remove initial strain, energy minimization (steepest descent) was performed on the initial configuration for 200 steps. The MD simulation was subsequently started involving an equilibration of 10 ps with initial velocities taken from a Maxwellian distribution at 315 K and meanwhile coupling the system to an external heat bath[21] at 315 K with time constant $\tau_s = 0.01$ ps. The volume of the system was kept fixed.

NVT Simulations. After equilibration another 290 ps was simulated under the following conditions: all covalent bond lengths as well as the water angle were constrained by the procedure SHAKE[21] (tolerance 0.000 01 nm), and a time step of 2 fs was used. The intermediate structures generated during MD were saved every 100 steps. The temperature was controlled by coupling to an external bath[21] at 315 K with time constant $\tau_s = 0.1$ ps. A twin-range cutoff for nonbonded forces of 0.8/1.0 nm was used; the pair list and forces for the range between 0.8 and 1.0 nm were updated every 10 steps. All dynamics simulations were run on a CONVEX C220 and C240 computer.

The series of additional simulations were performed starting with the configuration obtained after 300 ps of MD (A) as described above. For simulation A Ryckaert–Bellemans potentials[20] were used with modified methyl parameters.[33] Simulation A corresponds most closely with GROMOS using "hydrophobic" water oxygen (see Table II). Figure 2 gives an overview of all the simulations performed. We have studied the properties of several models with different van der Waals parameters for intermolecular potentials by only changing the Lennard-Jones parameter ϵ_{O-C} (models B to D), which are summarized in Table II. We simulated 200 ps for each of these models using the same conditions as for simulation A. Also in Table II, model E is represented. We performed this simulation to investigate the effect of the Lennard-Jones parameter σ on the properties of the interface. The Lennard-Jones parameters between oxygen and

TABLE II: Lennard-Jones and van der Waals Parameters between Water and Decane for the Different Models[a] as Well as for the Values Carpenter and Hehre[12] (CH), OPLS,[16] CHARMm[23] (CM), and GROMOS[17] (GR) Use

	A	B	C	D	E	CH[b]	OPLS[c]	CM[d]	GR[e]	GR[f]
A_{CH_3-O}	0.3724	0.2633	0.1974	0.0632	0.7017	0.9847				
A_{CH_2-O}	0.3091	0.2191	0.1638	0.0515	0.5824	0.8086				
C_{CH_3-O}	0.4230	0.2990	0.2242	0.0717	0.4320	0.5213				
C_{CH_2-O}	0.3511	0.2488	0.1861	0.0585	0.3511	0.4281				
ϵ_{CH_3-O}	1.201	0.849	0.637	0.203	0.637	0.690	0.682	0.694	1.319	0.700
ϵ_{CH_2-O}	0.997	0.706	0.529	0.166	0.529	0.566	0.560	0.551	1.163	0.617
σ_{CH_3-O}	0.310	0.310	0.310	0.310	0.344	0.352	0.353	0.372	0.312	0.346
σ_{CH_2-O}	0.310	0.310	0.310	0.310	0.344	0.352	0.353	0.367	0.319	0.354

[a] A_{ij} in 10^{-5} kJ nm^{12}/mol, C_{ij} in 10^{-2} kJ nm^6/mol, ϵ in kJ/mol, and σ in nm. [b] By combining ϵ and σ of SPC O atoms and OPLS[16] C atoms. [c] By combining ϵ and σ of OPLS C atoms with TIP3P[16] O atoms. [d] By combining ϵ and σ of CHARMm[23] C atoms and TIP3P O atoms. [e] GROMOS with hydrophobic water. [f] GROMOS with hydrophilic water.

carbon atoms used by Carpenter and Hehre[12] (CH), OPLS,[16] CHARMm,[23] and GROMOS[17] are listed in Table II for comparison.

NPT Simulations. When the repulsion between the C atoms of decane and the O atom of water was increased, the pressure in all spatial directions increased. Therefore, we performed four additional runs (A_p to D_p) with pressure scaling in the z direction (i.e., perpendicular to the interface) by coupling to a pressure bath[21] of 1 atm (time constant 0.5 ps), allowing the length of the box in this direction to change but keeping the box lengths in x and y directions fixed to their initial value in order to keep a stable interface. In this way the systems were allowed to adjust their bulk pressures by changing the volume of the box. Model A_p used the configuration obtained after 300 ps of simulation period of model A as its starting point, model B_p the last configuration of model B, model C_p the last configuration of model C, and model D_p the last configuration of model D. For the model A_p to D_p we simulated for a period of 200 ps (see Figure 2). For model E we did not perform a simulation with pressure scaling.

Pressure Calculations. By using the virial equation, we obtained the pressure tensor

$$P_{\alpha\beta} = \frac{1}{V}\left(\sum_{i=1}^{N} m_i v_{i\alpha} v_{i\beta} + \sum_{i=1}^{N-1}\sum_{j=i+1}^{N} F_{ij\alpha} r_{ij\beta}\right) \qquad (3)$$

$P_{\alpha\beta}$ is an element in the pressure tensor, α and β are the components (x, y, or z), V is the volume, m_i is the mass of particle i, $v_{i\alpha}$ is its velocity in the α direction, $F_{ij\alpha}$ is the α component of the total force on particle i due to particle j, and $r_{ij\beta}$ is the β component of the vector $\mathbf{r}_i - \mathbf{r}_j$. The kinetic contribution to the pressure is given by the first term in eq 3, and the virial contribution is given by the second. The three diagonal elements in the pressure tensor represent the relevant pressure components. We have used an atomic sum for the calculation of local pressures and a molecular sum for the calculation of the total pressure.[24] This choice will be discussed in further detail in another article.[25]

Surface Tension. The surface tension (γ) is defined, when the interface is perpendicular to the z axis,[26] as

$$\gamma = -\int (p'(z) - p)\, dz \qquad (4)$$

where $p'(z)$ is the lateral pressure, p is the bulk pressure, and the integral is defined over the boundary layer. The integral can be extended to infinity, because $p'(z) = p$ in the bulk phase. With two interfaces perpendicular to the z axis, as in our case, this gives

$$\gamma = -\frac{1}{2}\left(\frac{p_x + p_y}{2} - p_z\right) L_z \qquad (5)$$

in which $p_\alpha = P_{\alpha\alpha}$ ($\alpha = x, y, z$) and L_z is the (formal) box length in the z direction used for the calculation.

Free Energy. On a molecular dynamics time scale the penetration of water into the oil phase is not expected to be observed. To obtain the solubility of water in decane, we used the particle insertion method of Widom.[27] By randomly inserting the virtual particles into the bulk oil phase (using a grid) and averaging their local Boltzmann factors, the excess free energy of a water molecule ($\Delta\mu^{ex}$) in decane can be computed where $\mu^{wat/dec}$ is the free energy of a water molecule in bulk decane at a given reference

$$\Delta\mu^{ex} = \mu^{wat/dec} - \mu^{id} = -kT \ln \langle e^{-U_{pot}/RT} \rangle \qquad (6)$$

concentration (for which we choose the concentration of liquid water $c_{(l)}$), μ^{id} is the reference (i.e., the free energy of the water molecule in the ideal gas state at the same concentration $c_{(g)} = c_{(l)}$), and U_{pot} is the potential interaction energy that the inserted (ghost) particle experiences from the other (real) particles. The brackets denote an ensemble average. This method only works well at low densities where the number of successful insertions with low energies is large enough to converge within reasonable time to a stable value for the free energy. The particle insertions were performed over the last 100 ps of each simulation, using 500 insertions per configuration.

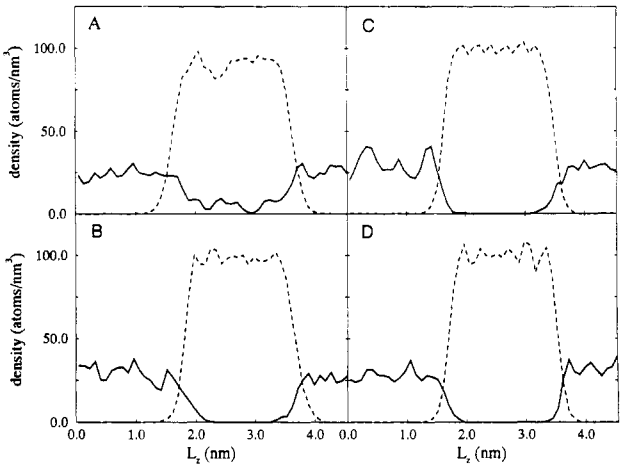

Figure 3. Density profiles with constant volume for the models (a) A, (b) B, (c) C, and (d) D. L_z is the box length. The dotted lines are the densities for water, and the solid lines for decane.

To obtain the free energy ($\Delta\mu$) with respect to a water molecule in bulk water ($\Delta\mu^{wat}$), the excess free energy of bulk water (μ^{wat}) with respect to the ideal gas state at same density as bulk water (μ^{id} at $c_{(l)}$) is needed. This can be expressed in the following way:

$$\Delta\mu^{ex} = \mu^{wat/dec} - \mu^{id} \quad (c_{(g)} = c_{(l)})$$

$$\Delta\mu^{wat} = \mu^{id} - \mu^{wat} \quad (c_{(l)}) \qquad (7)$$

$$\Delta\mu = \Delta\mu^{ex} + \Delta\mu^{wat}$$

$\Delta\mu^{wat}$ can be calculated in several ways, which will be discussed in the Results and Discussion Section. The $\Delta\mu$ can be used to calculate the solubility (S) expressed as the concentration ratio of water in decane ($c_{(sol)}$) and in liquid water ($c_{(l)}$)

$$S = \frac{c_{(sol)}}{c_{(l)}} = \exp\left(-\frac{\Delta\mu}{RT}\right) \qquad (8)$$

Orientation of Water. The orientation order of water molecules is defined as the cosine of the angle (θ_i) between the unit vector (μ) in the direction of the dipole and the unit vector normal to the interface ($\mathbf{n}_z$):

$$\cos\theta_i = \hat{\mu}\cdot\mathbf{n}_z \qquad (9)$$

Order Parameter. For the orientational preference of the decane molecules near the interface we calculated the order parameter S

$$S_{zz} = {}^1/_2(3\cos^2\theta_i - 1) \qquad (10)$$

where θ_i is the angle between the ith molecular axis and the interface normal (z axis) and where the bar implies averaging over time and molecules. The molecular axis is defined as the vector from C_{n-1} to C_{n+1}. Order parameters can vary between 1 (full order along the interface normal) and $-{}^1/_2$ (full order perpendicular to the normal), with a value of zero in the case of isotropic orientation.

Results and Discussion

Density Profiles. By calculating the density in 50 slabs parallel to the xy plane, we obtained density profiles. These density profiles for the decane/water system were obtained by averaging the time frames over the last 25 ps of the simulation period of all the

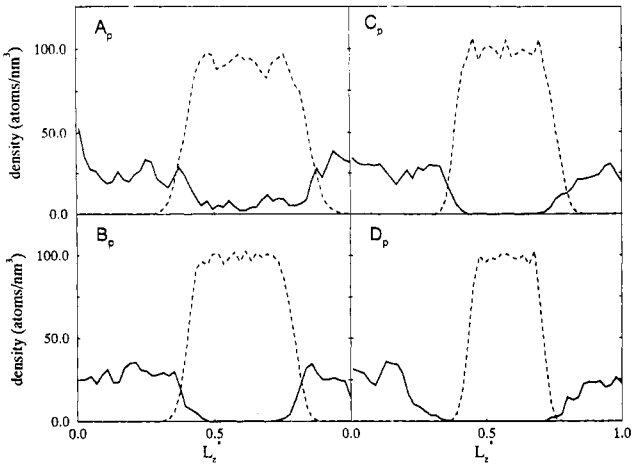

Figure 4. Density profiles with constant pressure in the z direction for the models (a) A_p, (b) B_p, (c) C_p, and (d) D_p. The dotted lines are the densities for water, and the solid lines for decane. The box length is normalized (L_z^*); the actual box length is shown in Figure 6.

models A to D. Figure 3 shows the density profiles for models A to D with constant volume. From the plots in Figure 3 it is obvious that if the van der Waals parameters were decreased, a sharper interface was formed. The values used in model A clearly resulted in a very wide interface, if not a mixed situation. We also observed a number of alkane molecules completely surrounded by water molecules as did Carpenter and Hehre, but only in model A. At the start of the A simulation there were two sharp interfaces, but the force field used clearly did not result in a molecularly sharp interface. Model B already showed a well-defined interface, but it was still too broad. The interface became sharper as the van der Waals parameters became even smaller (models C and D). We observed the same trend as Carpenter and Hehre did, in that the density of the alkane dropped much more slowly to zero than the water density. So movement of the decane molecules is likely to be more responsible for the sharper interface. Water molecules completely isolated in the decane phase were not observed. The van der Waals parameters used in model C are closest to the values used by Carpenter and Hehre, OPLS[16] and CHARMm[23] (also listed in Table II). However, we did not observe an interface of 1.0 nm width like Carpenter and Hehre: the interfaces obtained in our B, C, and D simulations were about 0.4–0.5 nm wide.

The density profile of model E is not presented in Figure 3, because this profile is almost identical compared to the profile of model C, indicating that the use of a larger $\sigma_{(CH_n-O)}$ ($n = 2$ or 3) does not have a large effect on the sharpness of the interface. According to the combination rule $\sigma_{ij} = (\sigma_i+\sigma_j)/2$, the σ's listed for model E in Table II are correct, whereas for models A to D only the ϵ between C atoms and O atoms were changed.

Since the models B to D appeared to have large bulk pressures (see Pressures subsection), we also performed simulations at constant pressures. The density profiles for the models A_p to D_p with constant pressure scaling only in the z direction are given in Figure 4. By adjusting the box length in the z direction, the densities of water and especially decane could relax. This also had some influence on the interface. The interface of model A_p is still mixed, but the interface of model B_p has become sharper with respect to model B, and the density of decane is more homogeneous. The plot for model C_p also shows a somewhat sharper interface. For model D_p an unusual interface is obtained with a "gap" between the water and decane phase, which was still increasing at the end of the simulation. In this case the virial of the total system was larger than the kinetic energy of the total system, and the box wanted to increase its volume. So the virial is too small to overcome the kinetic part of the pressure (see eq 3). This is not a real physical phenomenon but merely an artifact of the simulation.

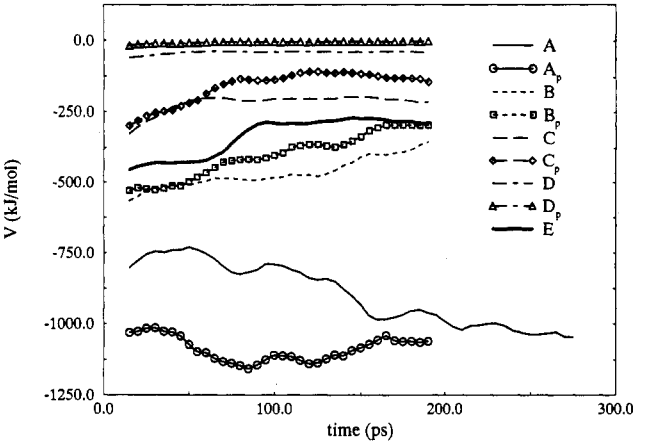

Figure 5. Interaction energies for the different models A to D_p plotted against simulation time.

TABLE III: Pressures[a] in the Three Spatial Directions and the Surface Tensions[b] for Models A to D_p

model	p_x	p_y	p_z	γ
A	−23 ± 6	−25 ± 7	−5 ± 6	42 ± 4
B	−14 ± 6	−14 ± 6	11 ± 6	58 ± 4
C	−2 ± 6	−1 ± 6	27 ± 6	65 ± 4
D	12 ± 6	12 ± 6	48 ± 6	83 ± 4
E	1 ± 6	2 ± 7	31 ± 6	66 ± 4
A_p	−18 ± 7	−17 ± 7	−1 ± 5	37 ± 4
B_p	−21 ± 6	−21 ± 6	0 ± 5	51 ± 4
C_p	−26 ± 6	−24 ± 6	−2 ± 5	57 ± 4
D_p	−21 ± 4	−21 ± 4	2 ± 4	72 ± 4

[a] p_x, p_y, and p_z in MN/m². [b] γ in mN/m.

Interaction Energy. In Figure 5 the interaction energies between decane and water are given to illustrate the effect of the change in intermolecular potentials on this energy. There is a clear trend of a decreasing interaction energy with respect to a decreasing intermolecular potential. Also, it can be seen that models A and A_p were not fully equilibrated, because the interaction energy did not converge, while the other models were equilibrated.

Pressures. Table III gives an overview of the pressure values for all the different models used. As the van der Waals parameters decreased, the pressures in all three directions increased in models A to D. Because of the large increase of the pressures, we performed the additional simulations A_p to D_p with pressure scaling in the z direction of 1.0 atm. The values in Table III for models A_p to D_p indicate a relaxation of all the pressures, and because of this relaxation the interface became sharper (see Figure 4b–d). For the models B_p and C_p this could be due to the fact that the partial volume of a decane molecule in water is smaller than the partial volume of a decane molecule in decane. Higher pressures in a constant volume would "force" the decane molecules into the water layer, resulting in a broader interface. By allowing the volume of the box to change, the pressures relax to a smaller value, and the decane molecules will return to their hydrophobic surrounding (and therefore increasing the volume of the box). The change in the volume of the box is illustrated in Figure 6, where the box length in the z direction is plotted against simulation time. This figure clearly shows a small decrease in box length (L_z) for model A_p (due to a negative P_z) and an increase of L_z for models B_p to D_p. The increase of L_z also implies that the total volume of the box increased, and therefore the density decreased. However, only the density of decane decreased; the density of the water phase remained (almost) constant. In the case of model D_p a very large increase in the first 50 ps of L_z occurred to compensate for the high pressures as listed in Table III. After approximately 50 ps, the increase rate is constant since the system is separated beyond the cutoff radii.

The pressures for model E are also listed in Table III, and the

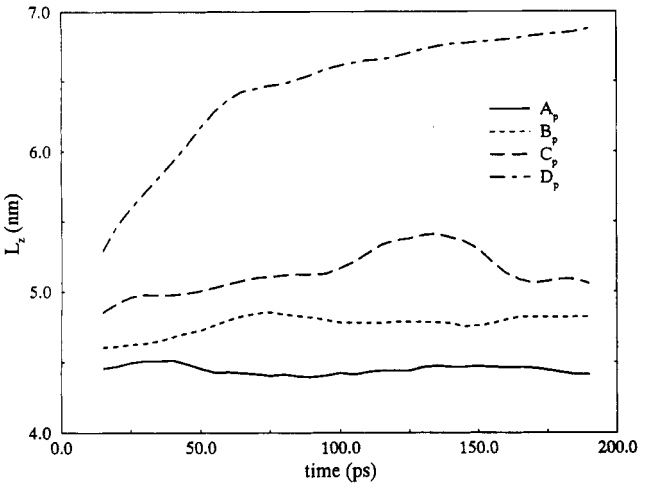

Figure 6. Box length in z direction (L_z) as a function of time for model A_p to D_p.

same trend can be seen as for the densities: the pressures in all three directions are similar for models C and E. Again, a larger σ between the C atoms of decane and the O atoms of water (but the same ϵ) does not give rise to a significant difference in properties.

Surface Tension. The experimental value for the surface tension between water and decane at 315 K is 48.2 ± 0.1 mN/m.[28] One should compare this value with the results obtained with the constant-pressure simulations. Without pressure scaling, the obtained surface tensions appeared to be higher due to higher lateral pressures. As can be clearly seen from Table III, the surface tension drops significantly in all simulations upon pressure scaling. Model A_p showed an average surface tension of 37 ± 4 mN/m, which was too small due to an interface that was too broad. If the surface tension becomes larger, the surface of the interface wants to decrease, and the two liquids prefer a more separated or demixed situation. This is the trend we observed in our simulations, and we can conclude that model D_p had an interface that is too sharp according to its surface tension, whereas models B_p and C_p showed an interface that was more in accordance with the experimental surface tension. It is obvious that lower values of ϵ_{O-C} are correlated with an increase in surface tension. In Figure 7 we plotted the lateral pressures for model C and model C_p to show the large decrease in the lateral pressures near the interface, which account for the actual surface tension. It is obvious from this figure (together with Figures 3c and 4c) that the position of the interface does not change when using pressure scaling, meaning that the water phase did not move or expand. The shift of the normal pressure toward P = 0.1 MN/m^2 (the pressure of the pressure bath we coupled to) is evident as well in Figure 7b.

TABLE IV: Free Energies[a] and Solubilities for Models A to C_p with SPC/E or SPC as a Reference

		SPC/E		SPC	
model	$\Delta\mu^{ex}$	$\Delta\mu$	S ($\times10^{-4}$)	$\Delta\mu$	S ($\times10^{-4}$)
A	−3.7 ± 0.2	18.7	7.9 ± 0.6	20.6	3.9 ± 0.3
B	−0.4 ± 0.2	22.0	2.3 ± 0.2	23.9	1.1 ± 0.1
C	+1.7 ± 0.2	24.1	1.0 ± 0.1	26.0	0.49 ± 0.04
D	+5.7 ± 0.4	28.1	0.22 ± 0.04	29.9	0.11 ± 0.02
E	+2.5 ± 0.2	24.9	0.74 ± 0.06	26.8	0.36 ± 0.03
A_p	−2.6 ± 0.4	19.8	5.2 ± 0.8	21.7	2.5 ± 0.5
B_p	−0.7 ± 0.4	21.7	2.5 ± 0.5	23.6	1.2 ± 0.2
C_p	+0.9 ± 0.4	23.3	1.4 ± 0.2	25.2	0.66 ± 0.1
expt		24.16	0.99	24.16	0.99

[a] Free energy in kJ/mol.

Water Ordering. In the bulk water the possibility to make hydrogen bonds with surrounding water molecules is very high, and the water molecules do not need to be oriented in a special manner to take optimal advantage of the possibilities to make hydrogen bonds. At the interfacial area this is not the case: the number of neighboring water molecules available for hydrogen bonds is smaller, and the water molecules orient themselves to create more possibilities for hydrogen bonding. The same behavior has been reported for the aqueous liquid/vapor interface,[4] the benzene/water interface,[9] and the hexane/water interface.[12] The ordering of the water molecules will be higher as the interface becomes sharper as was found in the simulations of water near a planar hydrophobic surface.[29] In fact, we observed a higher ordering of the water molecules near the interface as the van der Waals parameters were decreased (and the interface became sharper) as shown in Figure 8. Model D has the highest order and the sharpest interface. The ordering is not of a very long-range character: the water molecules were more ordered only just near the interface. It is interesting to see that the ordering is actually reversed: within the interface the dipole orientation is positive, which means that the H atoms are pointing toward the decane phase. Next to the interface the opposite orientation is observed over approximately two water layers.

Decane Ordering. In Figure 9 the order parameter of decane segments is plotted against the box length in the z direction relative to the interface at 1.6 nm. In the bulk the decane molecules are isotropically oriented ($S \approx 0$) in all simulations. As is to be expected, they are somewhat more laterally oriented (toward $S = -1/2$) near the interfaces, to ensure that the total surface of decane in close contact with water is as small as possible, although a fully lateral orientation was not observed. The decane molecules in model A did not show a more lateral orientation near the interface due to the broadness of the interface. Like the results for the ordering of water in Figure 8, there was almost no difference in lateral orientation for the decane molecules for models B to

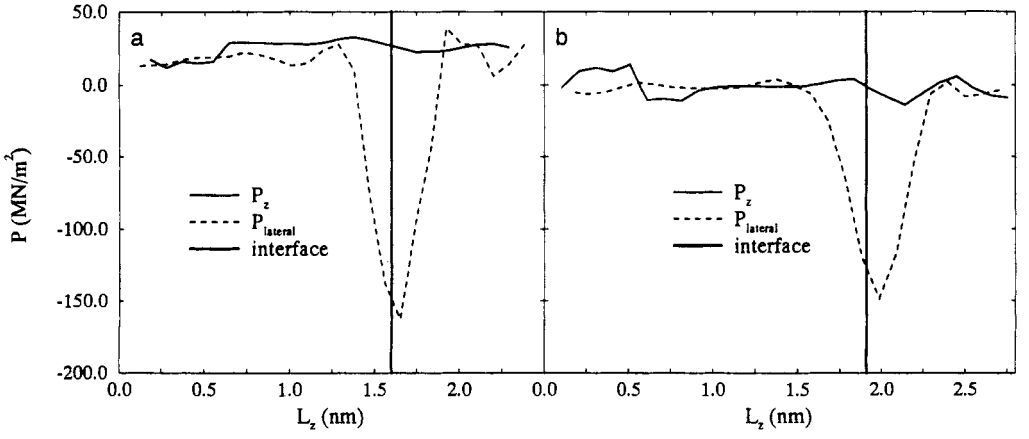

Figure 7. (a) Normal and lateral pressure against box length for model C and (b) for model C_p.

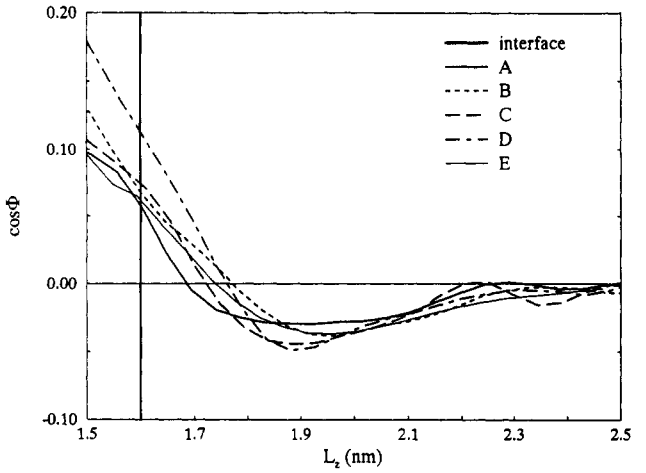

Figure 8. Orientation of the water molecules as a function of the box length in z direction (L_z). The interface is also plotted: it is placed at 1.6 nm and is an average taken from Figure 3a–d, where the density plots of decane and water intersect. The data in this plot are symmetrized for better statistics.

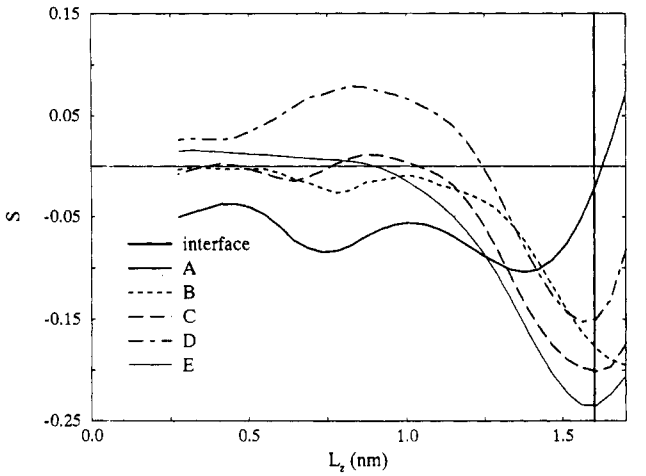

Figure 9. Order parameter for decane as a function of the box length in z direction (L_z). For legend see Figure 8.

E. Also clear from Figure 9 is that the decane molecules become more isotropically oriented in direct contact with the water molecules.

Free Energy. Table IV lists the free energies of SPC/E water in bulk decane for the models A to C_p as well as the corresponding solubilities. The experimental value for the free energy we calculated to be $\Delta\mu$ = 24.16 kJ/mol, using the solubility at 315 K of water in decane.[30] For the free energy of SPC/E in bulk SPC/E ($\Delta\mu^{wat}$) we used a value of 22.4 kJ/mol, derived from the value reported by Hermans *et al.*[31] of 6.4 kcal/mol, uncorrected for polarization, which we corrected by −1.25 kcal/mol for polarization[18] (we note that Hermans used a polarization correction of −0.9 kcal/mol, which disagrees with ref 18) and by +0.2 kcal/mol for a cutoff of 1.0 nm. The trend for the solubility of water in decane for the different models was obvious: the solubility decreased as the repulsion between the liquids increased. We also calculated the solubility for water in decane for three models with constant pressure, models A_p to C_p, to see whether the solubility would change with respect to their constant-volume counterpart. The solubility was comparable to their "parent" model: the solubility somewhat increased when performing pressure scaling, probably due to a small decrease in density of the decane phase. The values for S did not change drastically. Figure 10 shows the free energy versus the number of configurations used for the particle insertion. This figure clearly shows that the free energy converged to a constant value for all the models, so we performed a sufficient number of particle insertions.

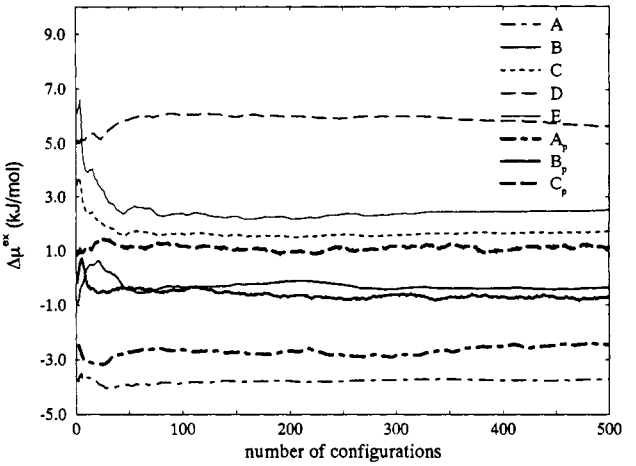

Figure 10. Free energy ($\Delta\mu^{ex}$) as a function of the number of configurations used for the particle insertion.

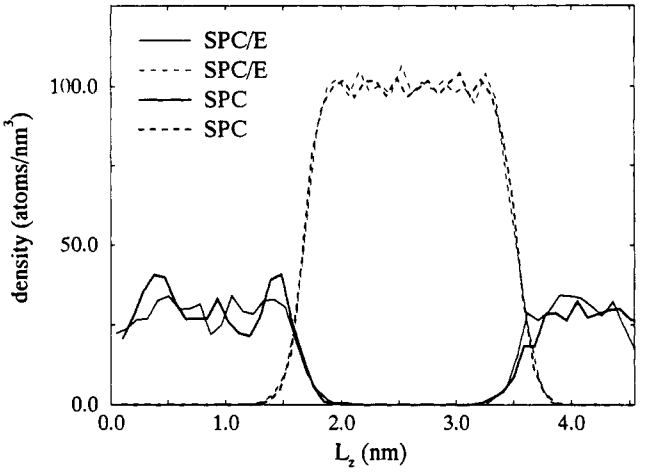

Figure 11. Density profiles (constant volume) for SPC/E and SPC water using the interaction potentials of model E.

The solubilities, for both model C and model E, were close to the experimental value of $S = 0.99 \times 10^{-4}$. When comparing this with the solubilities obtained in the constant-pressure simulations, model C_p has a somewhat higher solubility than model C. If we expect the same trend for a constant-pressure simulation of model E, the result will be very close to experimental for model E_p. So we conclude that the van der Waals parameters used in model E are accurate to simulate the interface between decane (or any other alkane) and water.

SPC/E vs SPC Water. We corrected the $\Delta\mu^{wat}$ for SPC/E for polarization; otherwise this $\Delta\mu^{wat}$ would be 27.6 kJ/mol (i.e., 6.4 + 0.2 kcal/mol for a cutoff of 1.0 nm[31]) instead of 22.6 kJ/mol. Compared to the $\Delta\mu^{wat}$ = 24.3 kJ/mol[31] of SPC, the uncorrected value is too high, resulting in a solubility for SPC/E in decane which is too low when comparing to SPC. When the correction on $\Delta\mu^{wat}$ for SPC/E is performed after the simulation, excellent solubility results are obtained. The problem is, however, that this correction on $\Delta\mu^{wat}$ cannot be made for the dynamical behavior at the interface during the MD run. A result from this is that the solubility of SPC/E in decane is expected to be too small in a dynamical equilibrium. SPC water needs no correction for the polarization. Besides, the chemical potential of SPC is very close to the experimental value.[31] Therefore, SPC is more suitable to be used for simulations at interfaces, since it will produce more realistic equilibrium distributions. We performed an extra simulation (200 ps) using the interaction potentials of model E and SPC water to investigate the dynamical behavior of SPC water at the interface with decane. The density profiles of SPC/E water and SPC water are presented in Figure 11: we observed no significant differences between the water profiles, even though

SPC has a higher solubility in decane compared to uncorrected SPC/E. The predicted solubilities with SPC as a reference become somewhat lower, however (Table IV). With SPC water the best model turns out to be model B. For model C_p the predicted solubility becomes 0.66×10^{-4}, which is still reasonable compared to the experimental value. We conclude that there is little difference between SPC and SPC/E but that SPC is to be preferred in dynamic simulations of interfaces.

Conclusion

The results reported in this paper show that the van der Waals parameters are of great importance when simulating the interface between two immiscible liquids. If the repulsion is not strong enough, the result is mixing of the two liquids at the interface, whereas too strong a repulsion leads to a situation where the surface tension is too large. The intermolecular potentials (as used in standard force fields like GROMOS and OPLS) for water and alkanes reproduce the properties of the bulk liquids correctly, but to describe the macroscopic properties of the interface between water and alkanes properly, the choice of a good combination of these intramolecular potentials is very important.

The sharpness of the interface changes enormously when the intermolecular van der Waals parameter ϵ is decreased. This also has a huge effect on the pressures in all spatial directions: the pressures increase rapidly when ϵ is decreased. The experimental value for the surface tension can be reproduced quite well for the decane/water system by only changing ϵ. The same holds for the solubility of water in decane.

At the interface, the structure of both water and decane is different from the bulk. Water has an orientational preference, because the number of hydrogen bonds per molecule is maximized. Decane has a more lateral orientation with respect to the interface. Both types of orientation do not change significantly when ϵ is decreased.

The combination of the Lennard-Jones parameters ϵ and σ to yield the exact values for the macroscopic properties between water and decane needs some further investigation. The Lennard-Jones parameters for water are well described in the literature, but the parameters for alkanes are probably not accurate enough. The use of special "hydrophobic" parameters for water oxygens in interaction with hydrophobic atoms, such as used in standard GROMOS,[17] cannot be recommended. To be able to describe the properties at the interface between water and any alkane accurately, better parametrization on alkanes is needed. It will also be needed to incorporate polarizability in the force field.

Without using explicit atomic polarizabilities, it is not possible to devise force field parameters that accurately predict both thermodynamic and dynamic properties. The best dynamics in the aqueous phase are obtained with the SPC/E model, but the best equilibrium distributions at the interface are obtained with the SPC model. With SPC/E the best interaction model is E ($\epsilon_{O-CH_3} = 0.637$ kJ/mol, $\epsilon_{O-CH_2} = 0.529$ kJ/mol and $\sigma_{O-C} = 0.344$ nm), with SPC the best interaction model is B ($\epsilon_{O-CH_3} = 0.849$ kJ/mol and, $\epsilon_{O-CH_2} = 0.706$ kJ/mol). The properties tested in this work are not very sensitive to the value of σ_{O-C}. We recommend the use of $\sigma_{O-C} = 0.344$ nm, also with the ϵ_{O-C}'s of model B, because this value follows from standard combination rules.

Finally, we note the effect of the use of different interaction models on systems other than alkane/water. We tested different models on the stability of a small α-helical peptide in water. In a previous simulation, using the "hydrophobic" parameters of GROMOS, this helix started to unfold after about 100 ps.[32] When using the "hydrophilic" GROMOS parameters in a 1-ns simulation, this unfolding started after approximately 800 ps. So there is a huge effect on the stability of the peptide when using the hydrophobic or hydrophilic interaction parameters of GROMOS.

Acknowledgment. This research was supported in part by Unilever Research Laboratory (URL), Vlaardingen, The Netherlands, and in part by the Foundation for Biophysics with financial aid from the Netherlands Research Organisation. We thank W. F. vanGunsteren (E.T.H., Zürich) for comments. The new GROMOS94 force field will contain corrected parameters.

References and Notes

(1) Croxton, C. A. *Statistical Mechanics of the Liquid Surface*; Wiley: New York, 1980.
(2) Lee, C. Y.; Scott, H. L. *J. Chem. Phys.* **1980**, *73*, 4591.
(3) Townsend, R. M.; Gryko, J.; Rice, S. A. *J. Chem. Phys.* **1985**, *82*, 4391.
(4) Wilson, M. A.; Pohorille, A.; Pratt, L. R. *J. Phys. Chem.* **1987**, *91*, 4873.
(5) Brodskaya, E. N.; Rusanov, A. I. *Mol. Phys.* **1987**, *62*, 251.
(6) Matsumoto, M.; Kataoka, J. *J. Chem. Phys.* **1988**, *88*, 3233.
(7) Benjamin, I. *J. Chem. Phys.* **1991**, *94*, 662.
(8) Pohorille, A.; Benjamin, I. *J. Chem. Phys.* **1991**, *94*, 5599.
(9) Linse, P. *J. Chem. Phys.* **1987**, *86*, 4177.
(10) Gao, J.; Jorgensen, W. L. *J. Phys. Chem.* **1988**, *92*, 5813.
(11) Smit, B. *Phys. Rev. A* **1988**, *37*, 3431.
(12) Locker Carpenter, I.; Hehre, W. J. *J. Phys. Chem.* **1990**, *94*, 531.
(13) Meyer, M.; Mareschal, M.; Hayoun, M. *J. Chem. Phys.* **1988**, *89*, 1067.
(14) Benjamin, I. *J. Chem. Phys.* **1992**, *97*, 1432.
(15) Berendsen, H. J. C.; Postma, J. P. M.; van Gunsteren, W. F.; Hermans, J. *Intermolecular Forces*; Pullman, B., Ed.; Riedel: Dordrecht, Holland, 1981; p 331.
(16) Jorgensen, W. L.; Madura, J. D.; Swenson, C. J. *J. Am. Chem. Soc.* **1984**, *106*, 6638.
(17) van Gunsteren, W. F.; Berendsen, H. J. C. Biomos b.v. Groningen.
(18) Marrink, S.-J.; Berkowitz, M.; Berendsen, H. J. C. *Langmuir*, in press.
(19) Berendsen, H. J. C.; Grigera, J. R.; Straatsma, J. P. *J. Phys. Chem.* **1987**, *91*, 6269.
(20) Ryckaert, J. P.; Bellemans, A. *Faraday Discuss. Chem. Soc.* **1978**, *66*, 95.
(21) Berendsen, H. J. C.; Postma, J. P. M.; van Gunsteren, W. F.; Di Nola, A.; Haak, J. R. *J. Chem. Phys.* **1984**, *81*, 3684.
(22) Ryckaert, J. P.; Ciccotti, G.; Berendsen, H. J. C. *J. Comput. Phys.* **1977**, *23*, 327.
(23) Brooks, B. R.; Bruccoleri, R. E.; Olafson, B. D.; States, D. J.; Swaminathan, S.; Karplus, M. *J. Comput. Chem.* **1983**, *4*, 187.
(24) Ahlström, P.; Berendsen, H. J. C. *J. Phys. Chem.*, in press.
(25) Ahlström, P.; Juffer, A. H.; Bekker, H.; Berendsen, H. J. C. To be published.
(26) Hill, T. L. *Introduction to Statistical Mechanics*; Dover: Mineola, NY, 1986; p 314.
(27) Widom, B. *J. Chem. Phys.* **1963**, *39*, 2802.
(28) Schmidt, M. Unilever Research Laboratory, Vlaardingen, The Netherlands, personal communication.
(29) Lee, C. Y.; McCammon, J. A.; Rossky, P. J. *J. Chem. Phys.* **1984**, *80*, 4448.
(30) Schatzberg, P. *J. Phys. Chem.* **1963**, *67*, 776.
(31) Hermans, J.; Pathiaseril, A.; Anderson, A. *J. Am. Chem. Soc.* **1988**, *110*, 5982.
(32) van Buuren, A. R.; Berendsen, H. J. C. *Biopolymers* **1993**, *33*, 1159.
(33) van der Ploeg, P.; Berendsen, H. J. C. *J. Chem. Phys.* **1982**, *76*, 3271.
(34) van der Ploeg, P.; Berendsen, H. J. C. *Mol. Phys.* **1983**, *49*, 233.
(35) Egberts, E.; Berendsen, H. J. C. *J. Chem. Phys.* **1988**, *89*, 3718.